

# Extension of the measurable temperature range of the LHD Thomson scattering system

メタデータ	言語: eng 出版者: 公開日: 2013-02-04 キーワード (Ja): キーワード (En): 作成者: Yamada, I., Narihara, K., Funaba, H., Yasuhara, R., Hayashi, H., Kohmoto, T. メールアドレス: 所属:
URL	<a href="http://hdl.handle.net/10655/9002">http://hdl.handle.net/10655/9002</a>

This work is licensed under a Creative Commons  
Attribution-NonCommercial-ShareAlike 3.0  
International License.



## Extension of the measurable temperature range of the LHD Thomson scattering system

I. Yamada, K. Narihara, H. Funaba, R. Yasuhara, H. Hayashi et al.

Citation: *Rev. Sci. Instrum.* **83**, 10E340 (2012); doi: 10.1063/1.4740525

View online: <http://dx.doi.org/10.1063/1.4740525>

View Table of Contents: <http://rsi.aip.org/resource/1/RSINAK/v83/i10>

Published by the [American Institute of Physics](http://www.aip.org).

---

### Related Articles

Optical tweezers with fluorescence detection for temperature-dependent microrheological measurements  
*Rev. Sci. Instrum.* **84**, 014103 (2013)

Construction and performance of a dilution-refrigerator based spectroscopic-imaging scanning tunneling microscope  
*Rev. Sci. Instrum.* **84**, 013708 (2013)

An apparatus for concurrent measurement of thermoelectric material parameters  
*Rev. Sci. Instrum.* **84**, 013907 (2013)

Chemical sensing by differential thermal analysis with a digitally controlled fiber optic interferometer  
*Rev. Sci. Instrum.* **84**, 015002 (2013)

Scanning tunneling microscope-quartz crystal microbalance study of temperature gradients at an asperity contact  
*Rev. Sci. Instrum.* **84**, 014901 (2013)

---

### Additional information on *Rev. Sci. Instrum.*

Journal Homepage: <http://rsi.aip.org>

Journal Information: [http://rsi.aip.org/about/about\\_the\\_journal](http://rsi.aip.org/about/about_the_journal)

Top downloads: [http://rsi.aip.org/features/most\\_downloaded](http://rsi.aip.org/features/most_downloaded)

Information for Authors: <http://rsi.aip.org/authors>

## ADVERTISEMENT



### MPS-SL Mechanical-Bearing Ball-Screw Linear Stages

- Compact 50-75 mm width with travel up to 100 mm
- Precision ground ball-screw or lead-screw drive
- DC servo or stepper motor
- Crossed-roller bearings
- High resolution (0.1  $\mu\text{m}$ ), repeatability ( $\pm 0.75 \mu\text{m}$ ) and accuracy ( $\pm 1.0 \mu\text{m}$ )
- High vacuum capable
- Compact multi-axis configurations



# Extension of the measurable temperature range of the LHD Thomson scattering system<sup>a)</sup>

I. Yamada,<sup>b)</sup> K. Narihara, H. Funaba, R. Yasuhara, H. Hayashi, and T. Kohmoto  
National Institute for Fusion Science, 322-6 Oroshi, Toki, Gifu 509-5292, Japan

(Presented 7 May 2012; received 7 May 2012; accepted 17 July 2012; published online 9 August 2012)

The large helical device Thomson scattering system was designed for the target electron temperature ( $T_e$ ) range,  $T_e = 50$  eV–10 keV. Above 10 keV, the experimental error becomes rapidly worse. In order to obtain reliable  $T_e$  data in the temperature range above 10 keV, we are planning to extend the measurable  $T_e$  range by following two methods. First we have installed one more wavelength channel that observes shorter wavelength region in polychromators. Next applying forward scattering configuration is another candidate. We estimate the data quality when the two methods are used. Both of the two methods are expected to improve  $T_e$  data quality at  $T_e \geq 10$  keV. © 2012 American Institute of Physics. [<http://dx.doi.org/10.1063/1.4740525>]

## I. INTRODUCTION

The large helical device (LHD) Thomson scattering system (TSS) measures electron temperature ( $T_e$ ) and density ( $n_e$ ) profiles along the LHD major radius. The LHD TSS was designed for the electron temperature range of  $T_e = 50$  eV–10 keV.<sup>1,2</sup> The data quality becomes worse rapidly in higher temperature region,  $T_e \geq 10$  keV. It is originated from the fact that the TS spectrum becomes wider than the wavelength region observed by our polychromator as shown in Fig. 2. In order to obtain reliable and accurate  $T_e$  data in high- $T_e$  plasma experiments, we tried several methods: guasi-simultaneous laser firing of three lasers and raw data summing methods. They have been successfully applied.<sup>3,4</sup> However, these methods have disadvantages too. For example, many lasers are needed for the guasi-simultaneous laser firing method, and many fixed plasma discharges (experiment time) are required for a raw data summing method. Therefore, we consider other methods to obtain reliable  $T_e$  and  $n_e$  data from a plasma discharge by using a laser. We are planning to extend the measurable  $T_e$  range by following two methods. First we have installed one more wavelength channel that observes shorter wavelength region in polychromators. Next forward scattering configuration, in which the TS spectrum becomes narrower than current backward scattering configuration, is another candidate. We estimate the data quality by using mock TS signal data when the two methods are applied. The mock data take some LHD plasma parameters into account, and TS spectrum are calculated by using Selden's formula.<sup>5,6</sup> In this paper, we describe the estimation of the  $T_e$  and  $n_e$  data quality at  $T_e \geq 10$  keV and discuss the extension of measurable temperature range of the LHD TSS.

## II. EXTENSION OF THE MEASURABLE $T_e$ RANGE

### A. Increasing polychromator channel

The original polychromators of the LHD TSS have five wavelength channels for observing Thomson scattered light in the wavelength region of 680–1050 nm, and a Rayleigh scattering calibration channel. In the filter selection, spectral response curves of all TS channels show a similar behavior above 10 keV then accurate determination of  $T_e$  becomes difficult in such high- $T_e$  region. To extend measurable  $T_e$  range, adding one more wavelength channel that observes shorter wavelength region is effective. Up to seven wavelength channels can be installed in the LHD polychromators as shown in Fig. 1. Then we have added the sixth TS channel for 20 polychromators that see the center plasma region. Figure 2 shows an example of spectral response of the polychromators. The reason why there is a gap between the fifth and sixth channels is to avoid the  $H\alpha$  line whose wavelength is 656.3 nm. Figure 3 shows estimated experimental errors in  $T_e$  and  $n_e$  when wavelength channels #1–#4, #1–#5, and #1–#6 are used in the data analysis. We note that the error estimations are carried out at electron density of  $5.0 \times 10^{19} \text{ m}^{-3}$  throughout this paper. In the LHD TS diagnostic, main error source has been found to be originated from shot noise in measured TS signals, the  $\delta T_e/T_e$  at different densities can be empirically estimated from  $\delta T_e/T_e \propto n_e^{-1/2}$ .<sup>3,4</sup> In the case where #1–#5 wavelength channels are used, the  $T_e$  error becomes rapidly larger

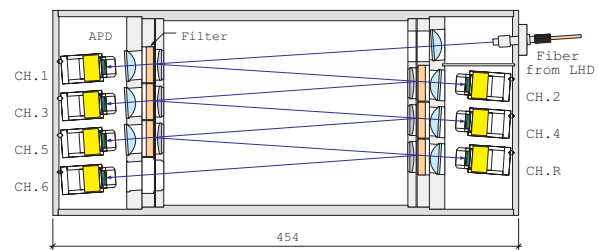


FIG. 1. Schematic diagram of the LHD 6 wavelength channel polychromator.

<sup>a)</sup>Contributed paper, published as part of the Proceedings of the 19th Topical Conference on High-Temperature Plasma Diagnostics, Monterey, California, May 2012.

<sup>b)</sup>Author to whom correspondence should be addressed. Electronic mail: yamadai@nifs.ac.jp.

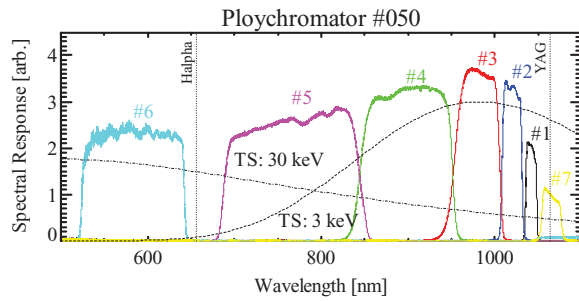


FIG. 2. Spectral response of the LHD 6 wavelength channel polychromator. Thomson scattering spectrum at  $T_e = 3$  keV and 30 keV are plotted.

above 10 keV, and reaches 100% at 50 keV. This agrees well with the experimental results. On the other hand, the  $T_e$  error is less than 10% even at 30 keV when the signal of the 6th channel is also taken into account. Concerning density error  $\delta n_e/n_e$ , the difference among the three cases is small, and all of them are less than 5%.

### B. Use of forward scattering configuration

Since the LHD TSS has a backward scattering configuration, TS spectral width and peak shift are greater than those in traditional right-angle scattering configuration TSS. When the forward scattering configuration where the laser beam direction is opposite is applied, The  $T_e$  error in the forward scattering configuration is expected to be smaller because a greater proportion of the TS spectrum is covered by the spectral range of this TSS, as shown in Fig. 4. Figures 5(a) and 5(b) show comparisons of estimated  $T_e$  and  $n_e$  errors respectively, in backward scattering and forward scattering configurations. In the estimation, wavelength channels #1–#5 were used. The scattering angle of the LHD TSS is  $163^\circ$  and  $17^\circ$  at the plasma center when the system is operating in backward and forward scattering configuration respectively. As expected, the forward scattering configuration is better for the temperature range above 5 keV, whereas it is not good for lower  $T_e$  range. When such forward scattering configuration is applied,  $T_e$  error,  $\delta T_e/T_e$  will be reduced less than 10% even at 50 keV. Concerning the  $n_e$  error, backward scattering configuration provides better result in almost whole region studied. Figures 6(a) and 6(b) show similar com-

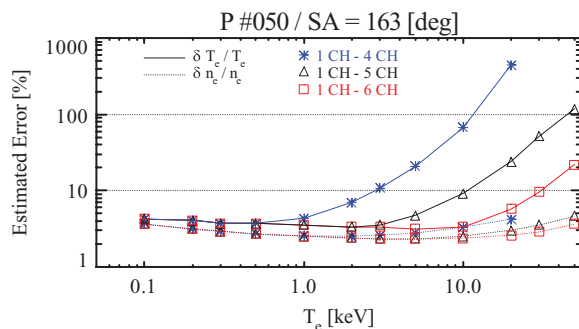


FIG. 3. Estimated  $T_e$  (solid curves) and  $n_e$  (dashed curves) errors. Crosses, triangles, and squares show  $T_e$  and  $n_e$  errors when wavelength channels #1–#4, #1–#5, and #1–#6 are used respectively.

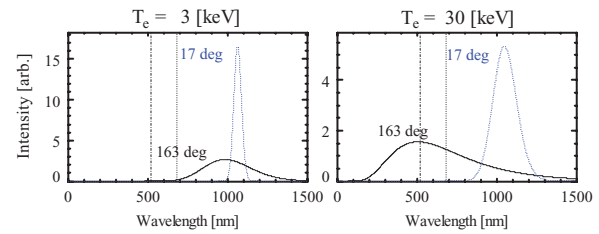


FIG. 4. Thomson scattering spectrum at  $T_e = 3$  and 30 keV, and the scattering angle of  $17^\circ$  and  $163^\circ$ . The broken and dashed lines show lower wavelength limits of the 5th and 6th channels respectively.

parisons when the wavelength channels #1–#6 are used in the determination of  $T_e$  and  $n_e$ .

Recently some multipath TS diagnostic systems have been developed to increase effective probing laser energy.<sup>7,8</sup> The laser beam after going through plasma is reflected by a mirror, and transmitted again in plasma. In these cases, the TS spectral shapes produced by the first and second pulses are the same. However, the spectrum significantly differs from each other in the LHD TSS as a result of the change in the scattering angle, as shown in Fig. 4. Therefore, TS signals from the first and second pulses may be required to be separately observed. For this, a long temporal delay path is needed between the first and second pulses. In our case, more than 10 m delay path is needed. Since it is not easy to install such long delay path in the LHD TSS, we consider that the mixed backward and forward scattering signals are observed. The red lines in Figs. 5 and 6 show the estimated  $\delta T_e/T_e$  error for the case where the mixed scattering pulses are observed without using a temporal delay path. From low temperature region to 1 keV, the  $\delta T_e/T_e$  error is in the same level as that obtained from the backward scattering signals. The mixing ratio of the backward and forward scattering configurations is assumed to be 100:100 in the calculation. Above 10 keV, the  $\delta T_e/T_e$  error is somewhat larger than that obtained from the forward scattering signals, however is significantly lower than that from the backward scattering signals. Therefore, it is expected that reliable  $T_e$  and  $n_e$  data can be also determined from mixed sig-

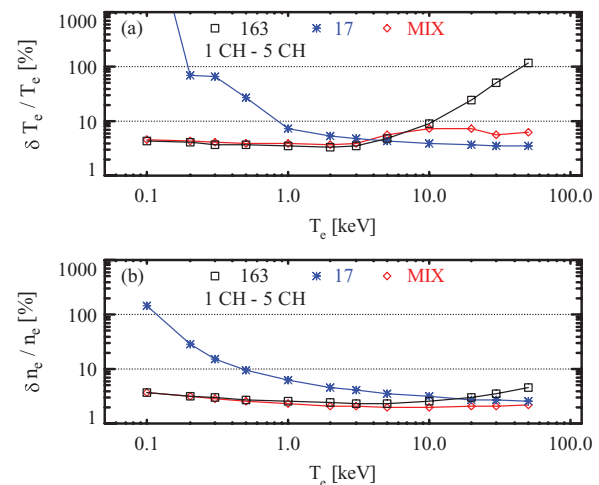


FIG. 5. Estimated  $T_e$  and  $n_e$  error when the wavelength channels #1–#5 are used for the backward scattering configurations, squares and forward scattering configurations, crosses. Diamonds show the result for the hybrid backward-forward scattering configuration.

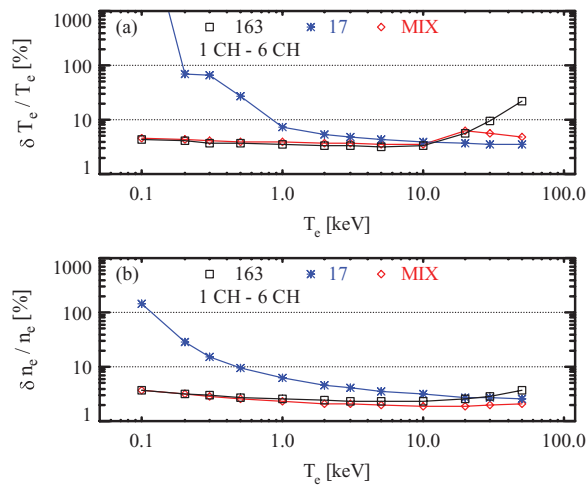


FIG. 6. Estimated  $T_e$  and  $n_e$  error when the wavelength channels #1–#6 are used.

nals. However, the mixing ratio will be changed from 100:100 in real experiments. For example, decrease in effective probing energy of the returned pulse due to misalignment of the return path may cause a systematic error. To estimate the systematic error, we studied the mixing ratio dependence of it, as shown in Fig. 7. In the calculation, we used data analysis table obtained on the assumption that the mixing ratio is 100:100, and mock TS signal data are generated at some mixing ratio. As expected, the systematic error becomes minimum at the ideal case of the mixing ratio of 100:100, and rapidly worse as the difference between the assumption and real situation becomes large. This result says that a proper data analysis table that takes real probing energy ratio of the incident and return paths into account should be used in the data analysis. It is noted that the ratio itself is not a major problem. If the ratio of the effective probing energies is 100:80, using the data analysis table calculated by using true ratio, 100:80, provides the best results.

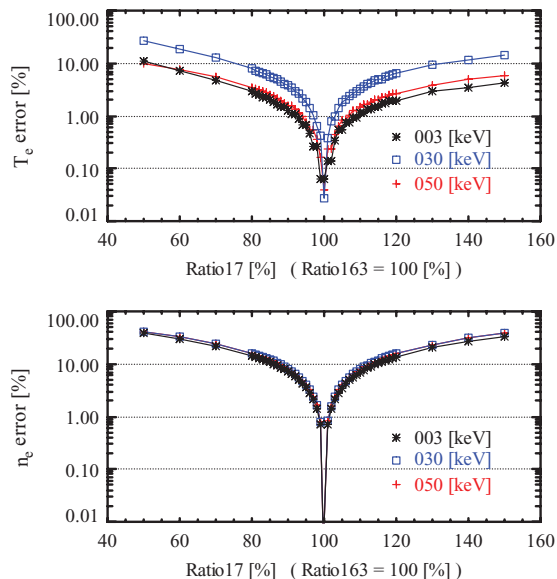


FIG. 7. Systematic errors in  $T_e$  and  $n_e$  obtained from the data analysis table produced on the assumption that the ratio163: ratio17 = 100:100.

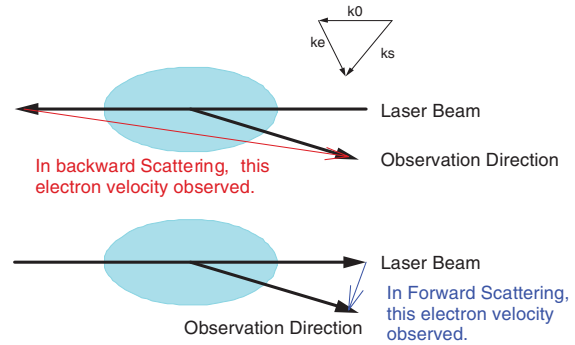


FIG. 8. In backward scattering configuration, parallel component to the laser beam of  $T_e$  is observed whereas vertical component is obtained in forward scattering configuration.

Finally we note that electron temperatures measured in the backward and forward scattering configurations is essentially different. Nearly parallel and vertical components of  $T_e$  are measured in backward and forward scattering configurations respectively, as shown in Fig. 8. Therefore a hybrid backward-forward TSS may be useful for not only extending measurable  $T_e$  range but also searching anisotropy of  $T_e$ .

### III. SUMMARY

We are planning to extend the measurable  $T_e$  range of the LHD TSS by two ways. One is adding one more wavelength channel that observes shorter wavelength region in polychromators, and the other is applying forward scattering configuration. We estimate the data quality by using mock data when the two methods are applied. Both of them will provide more accurate  $T_e$  data in high- $T_e$  region of  $T_e \geq 10$  keV. The  $T_e$  error will be reduced from 52% to 10% and 4% at  $T_e = 30$  keV by using the new polychromators and applying the forward scattering configuration respectively. It will be further reduced to 3.5% when both the methods are simultaneously applied.

### ACKNOWLEDGMENTS

This work was supported by the NIFS LHD project budgets (NIFS10ULHH005, NIFS10KCHH018, NIFS11ULHH005, and NIFS11KLEH007) and partially supported by the Grant-in-Aid for Scientific Research (C), No. 16540456.

- <sup>1</sup>K. Narihara, I. Yamada, H. Hayashi, and K. Yamauchi, *Rev. Sci. Instrum.* **77**, 1122 (2001).
- <sup>2</sup>I. Yamada, K. Narihara, H. Funaba, T. Minami, H. Hayashi, T. Kohmoto, and LHD experiment group, *Fusion Sci. Tech.* **58**, 345 (2010).
- <sup>3</sup>I. Yamada, K. Narihara, H. Funaba, H. Hayashi, T. Kohmoto, H. Takahashi, T. Shimozuma, S. Kubo, Y. Yoshimura, H. Igami, and N. Tamura, *Rev. Sci. Instrum.* **81**, 10D522 (2010).
- <sup>4</sup>I. Yamada, K. Narihara, H. Funaba, R. Yasuhara, T. Kohmoto, H. Hayashi, T. Hatae, H. Tojo, T. Sakuma, H. Yoshida, H. Fujita, and M. Nakatsuka, *J. Instrum.* **7**, C05007 (2012).
- <sup>5</sup>A. C. Seldin, *Phys. Lett. A* **79A**, 405 (1980).
- <sup>6</sup>J. Sheffield, *Plasma Phys.* **14**, 783 (1972).
- <sup>7</sup>T. Hatae, O. Naito, M. Nakatsuka, and H. Yoshida, *Rev. Sci. Instrum.* **77**, 10E508 (2006).
- <sup>8</sup>M. Yoshikawa, R. Yasuhara, M. Morimoto, Y. Shima, J. Kohagura, M. Sakamoto, Y. Nakashima, T. Imai, I. Yamada, K. Kawahata, H. Funaba, and T. Minami, *Rev. Sci. Instrum.* **83**, 10E333 (2012).